Water Science & Technology

Water Science & Technology Vol 00 No 0, 1 doi: 10.2166/wst.2022.271

Estimation of nitrous oxide emissions from rice paddy fields using the DNDC model: a case study of South Korea

Nadar Hussain Khokhar[a], Imran Ali[b], Hubdar Ali Maitlo[c], Naeem Abbasi[d], Sallahuddin Panhwar[a], Hareef Ahmed Keerio[e,*], Asim Ali[f] and Salah Uddin[a]

[a] Department of Civil Engineering, NUST Balochistan Campus, National University of Sciences and Technology, Quetta, Pakistan
[b] Department of Environment Sciences, Sindh Madressatul Islam University, Karachi, Sindh, Pakistan
[c] Department of Energy and Environment Engineering, Dawood University of Engineering and Technology, Karachi, Sindh, Pakistan
[d] Department of Bioresource Engineering, McGill University, Sainte-Anne-de-Bellevue, Quebec H9X 3V9, Canada
[e] Department of Environment Engineering, Quaid E Awam University of Engineering Science and Technology, Nawabshah 67450, Pakistan
[f] Department of Civil Engineering Technology, The Benazir Bhutto Shaheed University of Technology & Skill Development, Khairpur (Mir), Pakistan
*Corresponding author. E-mail: hareefkeerio@yahoo.com, hareefkeerio@hanyang.ac.kr

HAM, 0000-0002-8806-7714

ABSTRACT

The Denitrification-Decomposition (DNDC)-Rice is a mechanistic model which is widely used for the simulation and estimation of greenhouse gas emissions [nitrous oxide (N_2O)] from soils under rice cultivation. N_2O emissions from paddy fields in South Korea are of high importance for their cumulative effect on climate. The objective of this study was to estimate the N_2O emissions and biogeochemical factors involved in N_2O emissions such as ammonium (NH_4^+) and nitrate (NO_3^-) using the DNDC model in the rice-growing regions of South Korea. N_2O emission was observed at every application of fertilizer and during end-season drainage at different rice-growing regions in South Korea. Maximum NH_4^+ and NO_3^- were observed at 0–10 cm depth of soil. NH_4^+ increased at each fertilizer application and no change in NO_3^- was observed during flooding. NH_4^+ decreased and NO_3^- increased simultaneously at end-season drainage. Minimum and maximum cumulative N_2O emissions were observed at Chungcheongbuk-do and Jeju-do regions of South Korea, respectively. The simulated average cumulative N_2O emission in rice paddies of South Korea was 1.37 kg N_2O-N ha^{-1} $season^{-1}$. This study will help in calculating the total nitrogen emissions from agriculture land of South Korea and the World.

Key words: ammonium and nitrate, biogeochemical model, DNDC-Rice model, nitrous oxide, rice paddy

HIGHLIGHTS

- We successfully simulated N_2O emission from rice paddy fields of South Korea.
- DNDC model was used to estimate N_2O emission in South Korea.
- Biogeochemical factors of soil such as NH_4^+ and NO_3^- concentration were also focused upon.
- Simulated N_2O emission in this study was strongly correlated as $R^2 = 0.88$–0.90.
- Results may help to estimate the nitrogen budget of South Korea as well as the world.

GRAPHICAL ABSTRACT

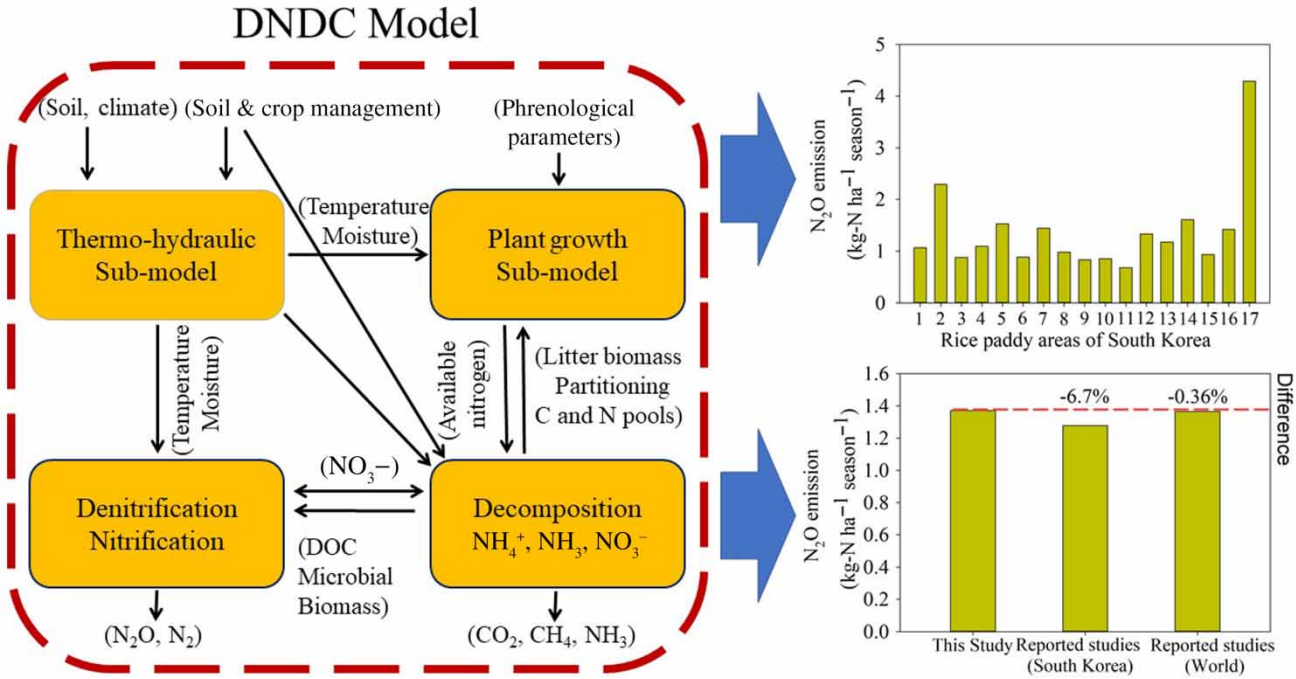

1. INTRODUCTION

Nitrous oxide (N_2O) is well known greenhouse gas for its global warming potential of 298 times greater than carbon dioxide (CO_2) (IPCC 2007). N_2O is also known for its role in damaging the stratospheric ozone layer (Fan *et al.* 2020). The soil ecosystem accounts for 65% (6.8 Tg N_2O-N $year^{-1}$) of the total N_2O emitted to the atmosphere mainly due to nitrogen fertilizer application (IPCC 2007). Nitrogen is the most deficient nutrient in soils and essential for plant growth. Nitrogen fertilizer is extensively used to meet the plant need and food demand at large. However, 1–5% of N fertilizer applied is lost into the atmosphere as N_2O emissions (Tang *et al.* 2018; Liu *et al.* 2019a). Nitrification and denitrification in the soil are core pathways of N_2O emissions (Wei *et al.* 2017; Duan *et al.* 2019). Nitrification occurs under aerobic conditions in which primary nitrifiers (*Nitrosomonas* sp.) oxidize ammonium (NH_4^+) to nitrite (NO_2^-) and NO_2^- is further converted to nitrate (NO_3^-) by secondary nitrifiers (*Nitrobacter* sp.) (Giguere *et al.* 2018; Chen *et al.* 2019b). Oxidation of ammonia leads to nitrification-driven N_2O emissions (Hu *et al.* 2015). Denitrification occurs under anaerobic conditions in which NO_3^- is stepwise transformed into N_2O and N_2 by facultative anaerobic bacteria (Xu *et al.* 2017; Giguere *et al.* 2018; Zhang *et al.* 2018a).

Rice (*Oryza sativa* L.) is cultivated on nearly 155 million ha around the world and feeds approximately 50% of the world's population (Fahad *et al.* 2019; Bashir *et al.* 2020). Paddy soils offer a diverse environment of biochemical cycles due to variation in water management practices (Kimura 2000). Nitrification occurs in the rhizosphere zone of paddy soils where nitrogen fertilizers release NH_3 (Wei *et al.* 2019; Yao *et al.* 2020). The NO_3^--N and NO_2^--N are stepwise transformed into N_2O and N_2 through the denitrification process (Ishii *et al.* 2009). A significant amount of N_2O is released from paddy soils to the atmosphere during the mid-season drainage period (Liu *et al.* 2019b; Liao *et al.* 2020). However, N_2O could be further transformed into N_2 during the anaerobic state of soils that creates an anaerobic environment in paddy soils (Abbas *et al.* 2019). N_2O emission during one growing season of rice paddy is estimated to be between 9 and 35 Gg N/year (Cai 2012). Previously, most studies have focused on N_2O emissions from agricultural soils, wetlands, and grasslands (Brenzinger *et al.* 2018; Zhang *et al.* 2019; Ogle *et al.* 2020; Žurovec *et al.* 2021). However, few studies have reported the N_2O emission from rice paddy at a national scale.

Recently, process-based models such as denitrification decomposition (DNDC) have been developed to add the feature of estimating N_2O emissions at a regional scale (Gaillard *et al.* 2018; Tian *et al.* 2018; Yue *et al.* 2019). Additionally, these models are able to accurately predict N_2O emissions under different agronomic management practices (Dutta *et al.* 2018;

Goglio *et al.* 2018; Jiang *et al.* 2020). The effect of climate change on crop yields can also be assessed using these models (Rafique *et al.* 2014; He *et al.* 2019). These models are frequently used for the identification of estimation factors of N_2O emissions (Gaillard *et al.* 2016; He *et al.* 2019). Different models such as DayCent, EPIC, CERES-EGC, and SWAT have been developed for these applications (Gaillard *et al.* 2018; Massara *et al.* 2018; Giltrap *et al.* 2020). At first, the DNDC model was explicitly developed for simulation and estimation of N_2O emissions, but now it has been further developed to include other ecosystems (Cui & Wang 2019; Yin *et al.* 2020; Zhao *et al.* 2020). The DNDC model can be used to simulate CO_2, CH_4, N_2O, NO, and NH_3 emissions (Shen *et al.* 2018; Jiang *et al.* 2020; Pandey *et al.* 2021). DNDC was previously used to estimate N_2O emissions from agricultural fields (Abdalla *et al.* 2020b; Jiang *et al.* 2021; Pandey *et al.* 2021), animal farms (Brown *et al.* 2001; Shen *et al.* 2019), and CH_4 emissions from paddy fields (Li *et al.* 2002; Wang *et al.* 2021b). This model connects ecological drivers such as soil properties, vegetation type, climate, and anthropogenic activities to soil and environmental variables. The links between these variables simulate transformation processes of organic carbon and nitrogen, through which CO_2, CH_4, N_2O, NO, and NH_3 are estimated (Camarotto *et al.* 2018; Zhang *et al.* 2018b; Li *et al.* 2019). The two operating modes of the DNDC model are site and regional modes. The site mode can simulate trace gas emissions at a particular site and therefore can be compared with field observations. The regional mode can estimate trace gas emissions from the entire region which is based on statistical uncertainty estimates.

Previously, specific site and treatment-oriented studies on N_2O emission from rice paddy fields have been reported in South Korea (Berger *et al.* 2013b; Kim *et al.* 2014a, 2016a; Pramanik *et al.* 2014). However, the present study is the first to estimate N_2O emission from rice paddy fields on a national scale in the Republic of Korea (South Korea) using the DNDC model. The objective of this study was to estimate N_2O emissions from rice-growing regions of South Korea and identify biogeochemical factors such as NH_4^+ and NO_3^- that are known to affect N_2O emissions. In this paper we will briefly show the preliminary results of a DNDC model of N_2O fluxes from 17 different rice paddy fields of South Korea.

2. MATERIALS AND METHODS

2.1. Region/site description and data collection

The official name of South Korea is the Republic of Korea (ROK), located in eastern Asia and covers the southern part of the Korean peninsula, which is located between the Sea of Japan (East Sea) in east, the Yellow Sea in west, and the Korea Strait, a sea passage between South Korea and Japan in the south. South Korea shares a land border with North Korea in north. The country also shares maritime borders with China and Japan (Macdonald & Clark 2018). The total area of South Korea is 99,678 km² the country is about the size of Iceland, or slightly smaller than the United States' State of Pennsylvania (You 2009). South Korea is divided into six provinces namely Chungcheongbuk-do, Chungcheongnam-do, Gyeongsangbuk-do, Gyeongsangnam-do, Jeollabuk-do, and Jeollanam-do, one autonomous province Jeju-do, six metropolitan cities namely Busan, Daegu, Daejeon, Gwangju, Incheon, and Ulsan. Seoul is the capital city of the country. South Korea has a population of 50.8 million inhabitants in 2016. The official language is Korean. Forests cover 64% of the total land area in South Korea (Lee *et al.* 2019). Rice is the most important crop here, accounting for about 90% of the country's total grain production and over 40% of farm income. Barley, soybeans and potatoes are the other major broad acre crops. Fruit, particularly citrus, and vegetables are also widely grown (Neszmelyi 2017).

N_2O emissions were estimated from 17 rice-growing regions across South Korea, as shown in Table 1. To compile data sets on different management practices of agricultural systems such as (1) soil properties, (2) irrigation, and (3) fertilizer application we referred to reported studies on a rice paddy fields in South Korea as shown in Table 2, and supplementary materials Tables S1, and S2, respectively. Reported agronomic practices varied slightly such as date of sowing, fertilizer application, irrigation, and harvesting were different. For missing data on input parameters, we used average values as prevalent in the region. The date of sowing was 12-06-2019 and the date of harvesting was 18-10-2019. Based on data available in Table 2 we selected soil texture silt loam, average bulk density, soil pH, and soil organic carbon as 1.17 g cm^{-3}, 6.2, and 0.0201 (kg $C{\cdot}kg^{-1}$), respectively. The date of flooding and the date of end-season drainage were selected from Table S1 and was 11-06-2019 and 29-09-2019, respectively. The dates of fertilizer application at different growing stages of the crop such as basal, tillering, and panicle stage were 11-06-2019, 29-06-2019, and 23-07-2019, respectively (Table S2). Climatic characteristics of each region, such as minimum and maximum temperature, precipitation, wind speed, solar radiation, and air humidity, were collected from Korean metrological administration reports 2019 (KMA 2019).

Table 1 | Cultivated area of rice paddies in different regions of South Korea (KOSIS 2019)

Site order	City/Province	Total arable area (ha)	Rice paddy area (ha)	Rice paddy area (%)
1	Seoul	149	131	87.9
2	Busan	2,503	2,383	95.2
3	Daegu	3,560	2,970	83.4
4	Incheon	11,610	10,419	89.7
5	Gwangju	5,302	4,988	94.1
6	Daejeon	1,259	1,109	88.1
7	Ulsan	4,402	4,102	93.2
8	Sejong	4,226	3,970	93.9
9	Gyeonggi-do	88,586	78,484	88.6
10	Gangwon-do	39,643	29,710	74.9
11	Chungcheongbuk-do	43,846	35,069	80.0
12	Chungcheongnam-do	143,288	134,035	93.5
13	Jeollabuk-do	136,294	118,340	86.8
14	Mr	186,954	161,442	86.4
15	Gyeongsangbuk-do	113,413	99,551	87.8
16	Gyeongsangnam-do	77,640	67,895	87.4
17	Jeju-do	6,562	113	1.7
	Total	869,236	754,713	86.8

Table 2 | Soil and crop parameters for denitrification and decomposition model

Order	Region	GPS coordinates	Year	Sowing	Harvesting	Soil texture	Soil pH	SOC (kg C/kg)	BD (g/cm^3)	Reference
1	Chung-buk	NA*	2000	12-Jun	04-Oct	NA*	5.9	0.0379	NA*	Ok *et al.* (2011)
2	Gimje	36°44′E;127°52′N	2012–13	21-Jun	20-Oct	Silt loam	5.6	0.0323	NA*	Chun *et al.* (2016)
3	Jinju	36°50′N;128°26′E	2006–7	10-Jun	20-Oct	Clay loam	6.1	0.0384	1.1	Ali *et al.* (2008)
4	Jinju	36°50′N;128°26′E	2011–12	10-Jun	20-Oct	Silt loam	6.9	0.0085	NA*	Haque *et al.* (2016)
5	Jinju	35°08′N;128°05′E	2010	08-Jun	21-Oct	Fine silty, mixed	6.6	0.015	NA*	Kim *et al.* (2013)
6	Jinju	35°08′N;128°05′E	2009–10	15-Jun	15-Oct	Fine silty, mixed	6.6	0.0098	NA*	Kim *et al.* (2012)
7	Jinju	35°06′N;128°07′E	2007–11	15-Jun	15-Oct	Fine silty, mixed	6.2	0.0144	NA*	Kim *et al.* (2016b)
8	Jinju	35°06′N;128°07′E	2011–12	15-Jun	15-Oct	Fine silty, mixed	6.32	0.0144	NA*	Kim *et al.* (2014b)
9	Jinju	36°50′N;128°26′E	2011	11-Jun	21-Oct	Silt loam	6.2	NA*	NA*	Pramanik *et al.* (2013)
10	Jinju	36°50′N;128°26′E	2014	11-Jun	21-Oct	Silt loam	6.32	0.011	NA*	Pramanik & Kim (2014)
11	Milyang	36°36′N;128°45′E	2008	05-Jun	20-Oct	Silt loam	5.98	0.023	1.23	Lee *et al.* (2010)
12	Sacheon	35°08′N;128°05′E	2010–11	12-Jun	24-Oct	Silty clay loam	6.6	0.0169	NA*	Gutierrez *et al.* (2013)

NA*Data not available.

2.2. DNDC-Rice model description

The DNDC-Rice model has three main segments: (1) soil climate, (2) crop growth, and (3) biogeochemistry of soil. The scientific aspects and background information of this model are explained by Fumoto *et al.* (2008). The DNDC model is a process-based computer simulation model based on carbon and nitrogen biogeochemistry that was originally developed to estimate N_2O emissions in agroecosystems. The model is based on two important components such as physicochemical and

biochemical components. The physicochemical component includes (soil climate, crop growth, and decomposition sub-models) that predicts the redox potential, pH, soil temperature, soil moisture, and substrate concentration profiles driven by ecological drivers such as climate, soil, vegetation, and anthropogenic activities. The biochemical component includes nitrification, denitrification, and fermentation sub-models and predicts the gas emissions from plant–soil systems such as carbon dioxide, nitrous oxide, nitric oxide, dinitrogen, methane, and ammonia (Wang *et al.* 2022).

All the input factors in each component of the DNDC-Rice model are reported in Fumoto *et al.* (2010). The soil climate simulates the functions of moisture, temperature, and O_2 in the soil layers (0–50 cm depth) and it also simulates the greenhouse gases based on physicochemical properties of soil, daily weather, and agronomic practices. The movement of oxygen in undisturbed soil cores of croplands was explained with Buckingham–Burdine–Campbell diffusion model (Osozawa & Kubota 1987). The crop growth in the DNDC-Rice model is simulated with the computer program MACROS modules (Penning de Vries *et al*. 1989). In the crop growth section, nitrogen availability, the atmospheric concentration of CO_2, respiration of soil, and allocation of C are considered as main components of the photosynthesis process of a plant (Zhang & Niu 2016). The fluxes of carbon from rice paddy roots to soil are assessed as a part of the C balance. In soil biogeochemistry section, different biogeochemical processes are simulated as a part of soil and environmental properties. The organic carbon decomposition is assessed with first-order reaction kinetics, where the controlling factors are soil water content, temperature, proportion of clay content, concentration of O_2, nitrogen deficiency, and soil tillage. In this section, hydrogen (H_2) and dissolved organic carbon (DOC) production is calculated under anaerobic conditions. Both H_2 and DOC are worked as electron donors for the reduction of oxidants such as Mn^{4+}, Fe^{3+}, and SO_4^{2-} while helping in the production of CH_4. When paddy soil is drained, both oxidants and CH_4 are oxidized by atmospheric O_2 diffusion into paddy soil and results in N_2O emissions.

2.3. N_2O sampling and validation of the model output

The simulated results of this study were validated using the experimental records of field studies conducted in South Korea as published previously (Berger *et al.* 2013a; Kim *et al.* 2014a). The same procedure of validation of DNDC simulations was adopted by Cai *et al.* (2003) and Fumoto *et al.* (2008). Berger *et al.* (2013a) conducted field experiments and N_2O flux measurements that were done between 11 May 2010 and 23 October 2010 at the FDFM paddy and between 6 May and 15 September 2011 at all three paddies. To measure N_2O exchange at the soil–water/atmosphere interface, closed-chamber measurements in conjunction with a photoacoustic infrared gas analyses (Multigas Monitor 1312, INNOVA, Ball-erup, Denmark) was used every 2 days at each experimental site. One day before the measurement, eight polyvinylchloride (PVC) cylinders (20 cm long and 19.5 cm wide) were installed 6 cm deep in the soil, so that depending on the water level of the rice paddy they poked out of the paddy water at least 2 cm. At each rice paddy, four of them contained rice plants, the other four were installed on spots without rice plants. For the measurement days, the cylinders were connected to chambers with a tubing connection to the gas analyzer, which determined the N_2O concentration of the chamber's headspaces after 0, 8, 16, 24, and 36 min. The reproducibility of one single N_2O concentration measurement was ± 32 ppb. From a linear increase or decrease of the N_2O concentration in the chambers' headspaces the N_2O flux was calculated considering the total chamber volume of the gas analyzing system, including the chamber head-space volume, volume of the two 25 m long Teflon tubes and of the CO_2 and H_2O gas traps. Cumulative N_2O emissions were calculated by multiplying the N_2O emission rates of 2 consecutive measurement days with the corresponding time period. These time-weighted N_2O flux means were then summed up over the measurement period.

Kim *et al.* (2014a) conducted a field experiment in which rice cultivation experiments were carried out at the National Academy of Agricultural Science Research Farm (37°15′N; 126°59′E; 12 m elevation), Rural Development Administration, Suwon, Korea, in 2008. Methane and N_2O emission characteristics were investigated during the rice cropping season using the closed-chamber method (Rolston 1986). In each plot, three transparent acryl chambers (width 62 cm, length 62 cm, and height 112 cm) were placed permanently into the soil after transplanting the rice seedlings. There were four holes in the bottom of each chamber to control the amount of floodwater. The chamber was equipped with a circulating fan to ensure complete gas mixing during the period of sampling. Eight rice plants were covered by each chamber. Gas sampling was carried at 11:00–13:00 to determine the average daily N_2O emission rates during the cropping season. Briefly, gas samples in triplicates were collected once a week using 50-mL air-tight plastic syringes at 0-, 15-, and 30-min intervals after manually closing the chamber. The collected gas samples were transferred into 30-mL air-evacuated glass vials sealed with a butyl rubber septum. Nitrous oxide concentrations were determined using gas chromatograph (Shimadzu, GC-2010) with a stainless-steel column packed with Porapak Q column (Q 80–100 mesh) and equipped with a 63 Nielectron capture detector.

The temperatures of the column, injector, and detector were adjusted at 70, 80, and 320 °C, respectively. Helium and hydrogen gases were used as the carrier and burning gases, respectively.

2.4. Statistical analysis

The SPSS Statistics 20 software package was used for analysis. The Pearson correlation test was performed to determine the correlation between simulated and observed N_2O emission.

3. RESULTS AND DISCUSSION

3.1. Climatic factors

Climatic factors of all regions used in the DNDC model were averaged as shown in Figure 1 Average solar radiation, humidity, wind speed, minimum temperature, maximum temperature, and precipitation during the rice-growing season were 15.5 Mj m^{-2} day^{-1}, 74.7%, 2.1 m s^{-1}, 20.2 °C, 28.2 °C, and 6.1 mm m^{-2} day^{-1}, respectively. Annual average climatic factors were significantly lower than during the growing season except for wind speed and solar radiation. Annual average solar radiation, humidity, wind speed, minimum temperature, maximum temperature, and precipitation during the rice-growing season were 14.2 MJ m^{-2} day^{-1}, 63.3%, 2.2 m s^{-1}, 9.5 °C, 18.8 °C, and 2.8 mm m^{-2} day^{-1}, respectively.

3.2. Comparison between observed and simulated N_2O emissions to validate the results of DNDC model

Since the DNDC model simulates N_2O emission based on available data of soil climate, crop growth, and biogeochemistry of soil, to validate the simulated results it is therefore very necessary to compare the results with N_2O emission observed in the field. Observed N_2O emissions were compared with simulated emissions from rice paddies to evaluate the performance of the DNDC-Rice model (Figure 2). Observed N_2O emissions in 2010 during rice paddy growing season ranged from −21.5 to 87.4 μg m^{-2} h^{-1} while the simulated values were in the range of −15.4 to 78.1 μg m^{-2} h^{-1} (Figure 2(a)). However, the difference between observed and simulated results of N_2O emission is not significant in this study. The N_2O emission from paddy fields vary due to soil water content, thermal regime, soil organic matter, and nitrogen fertilizer application (Xing *et al.* 2009; Pandey *et al.* 2014; Xu *et al.* 2020). In this study, the slight difference in soil water content and nitrogen fertilizer application reflected in change in N_2O emission. In 2008, minimum observed and simulated N_2O emissions were 0.03 and 2.8, respectively while maximum observed and simulated N_2O emissions were 54.2 and 50.5, respectively (Figure 2(b)). The difference between simulated seasonal emissions and observed emissions was 5.0% and 6.4% in 2010 and 2008, respectively. A similar pattern between simulated and observed N_2O emission was reported (Abdalla *et al.* 2010). The simulated N_2O emission was positively correlated with observed N_2O emission in 2010 ($R^2 = 0.96$, $n = 45$) (Figure 3(a)). Similarly, the simulated N_2O emission in 2008 was positively correlated with observed N_2O emission ($R^2 = 0.90$, $n = 34$) (Figure 3(b)). Thus, the DNDC model successfully simulated N_2O emissions at sites one and two. Wu & Zhang (2014) Reported ($R^2 = 0.892$, $n = 28$, $p = 0.01$) consistency between observed and simulated N_2O emissions from paddy fields under water-saving irrigation. Correlation between observed and simulated seasonal N_2O fluxes from different sites was reported as $R^2 = 0.93$, $n = 9$, $P<0.01$ (Babu *et al.* 2006). Another correlation between observed and simulated N_2O fluxes were reported $R^2 = 0.75$ (Bhanja *et al.* 2019).

3.3. N_2O emissions in different regions of South Korea

Rice paddies were cultivated in 17 different regions of South Korea as shown in supplementary material Figure S1. Rice paddies are cultivated on 754,713 hectares that correspond to 87% of the total arable land of South Korea (Table 1). A maximum 161,442 hectares of rice paddies was cultivated in Jeollanam-do and a minimum of 113 hectares in Jeju-do. In each region N_2O emission was observed only at basal, supplementary one, and supplementary two fertilizer applications and after end-season drainage. N_2O emission after the dates of basal N fertilizer application was reported (Chen *et al.* 2019a). N_2O emission was not observed between all three fertilizer applications. It was also not observed between supplementary fertilizer two and end-season drainage. Oxidation and reduction take place in paddy fields. The application of ammonium N containing fertilizers is nitrified in the oxidized layer, at the water–soil interface, forming nitrate, which moves downwards and denitrified in the reduced layer, producing N_2O. In the presence of a water layer on the soil N_2O is further reduced and escapes to the atmosphere as N_2. N_2O is emitted mainly through the soil surface in the absence of floodwater (Xing *et al.* 2009; Majumdar 2013; Wu *et al.* 2022). Since there was continuous flooding between three fertilizer applications and

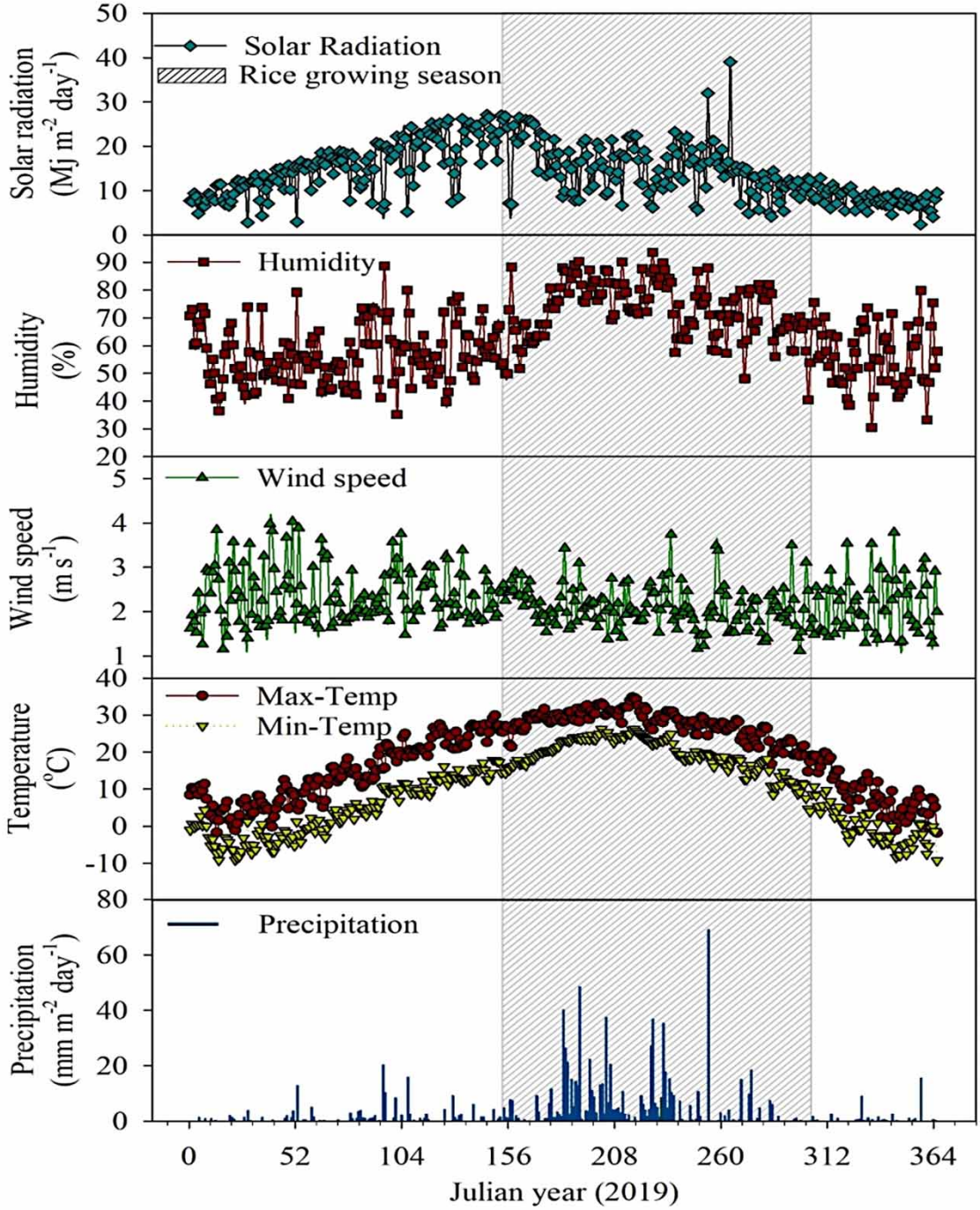

Figure 1 | Average climatic factors of rice paddy regions of South Korea.

between supplementary fertilizer and end-season drainage N_2O was further reduced and escaped to the atmosphere as N_2, therefore N_2O emission was not observed during these periods of the growing season. Minimum and maximum N_2O emission were observed at basal fertilizer application and after end-season drainage, respectively. N_2O emission varied significantly due to the change in climatic factors and physicochemical properties of each region. The continuous flooding, periodic drainage, seasonal tillage, and other agricultural activities during the rice-growing season make paddy soils in a state of dry–wet alternation (Liao *et al.* 2020; Zuo *et al.* 2022). Consequently, different soil layers have different

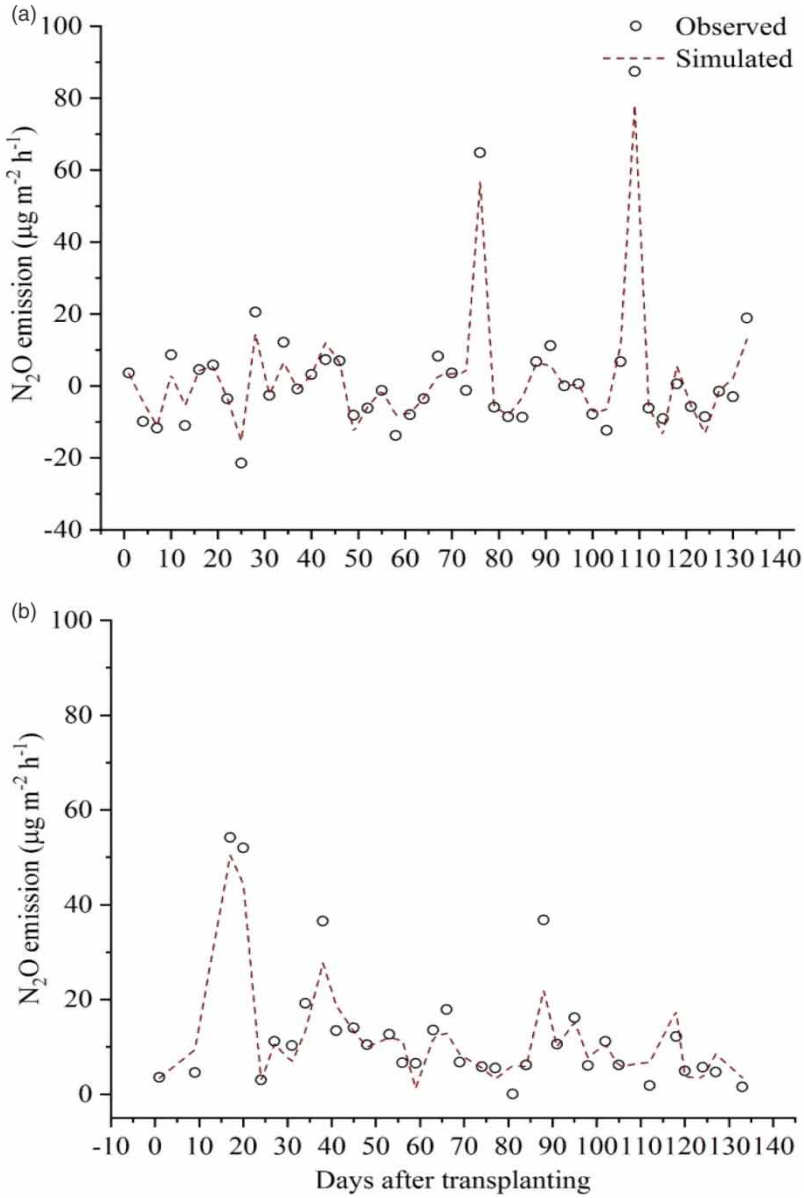

Figure 2 | (a) Observed and simulated seasonal patterns of N_2O emission in 2010 (Berger *et al.* 2013a), (b) N_2O emission in 2008 (Kim *et al.* 2014a). (The observed values were digitized from the above-mentioned publications using Origin software.)

water content and aeration statuses, leading to the changes in chemical composition such as soil redox, pH, state of nitrogen, and other properties in time and space (Wang *et al.* 2021a; Zuo *et al.* 2022). In addition, environmental changes such as the changes in soil moisture, temperature, can affect the composition of soil microbial communities, thus, in turn, affecting the nitrification and denitrification of soil that may further lead to either increases or decreases in N_2O emission (Wang *et al.* 2017; Qin *et al.* 2020).

N_2O emission from rice paddy fields of all regions was averaged as shown in Figure 4. Average N_2O emissions at basal, supplementary-one and supplementary-two fertilizer applications were 12.2 ± 1.5, 2.7 ± 0.81, and 52.1 ± 3.7 μg m^{-2} h^{-1}, respectively. Maximum N_2O emission $2{,}518.3 \pm 225$ was observed on the first day of end-season drainage Figure 4(b). N_2O emission decreased gradually after end-season drainage until the last day of N_2O simulation. Maximum 79% N_2O emission of the entire season occurred following end-season drainage when soil is dry and creating suitable conditions for nitrification and denitrification (Adviento-Borbe *et al.* 2015; Abdalla *et al.* 2020a).

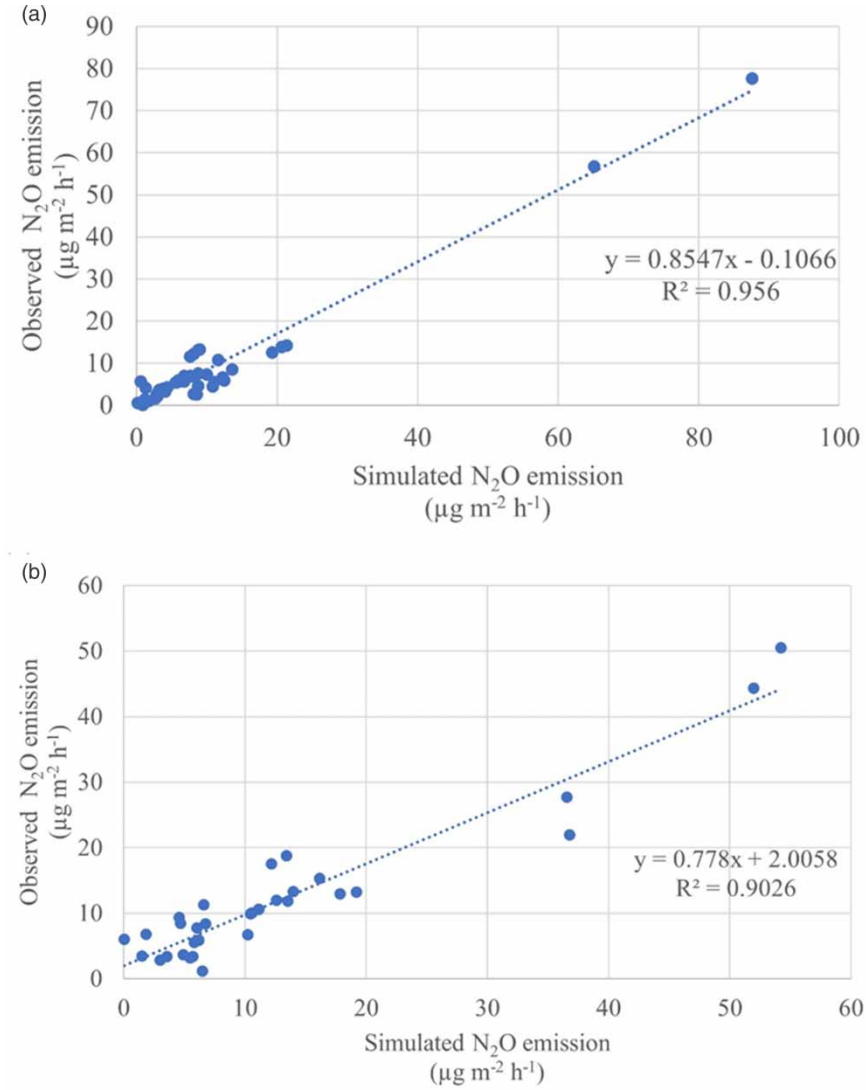

Figure 3 | (a) Correlation between observed and simulated N_2O emission in 2010 (Berger *et al.* 2013a), (b) Correlation between observed and simulated N_2O emission in 2008 (Kim *et al.* 2014a).

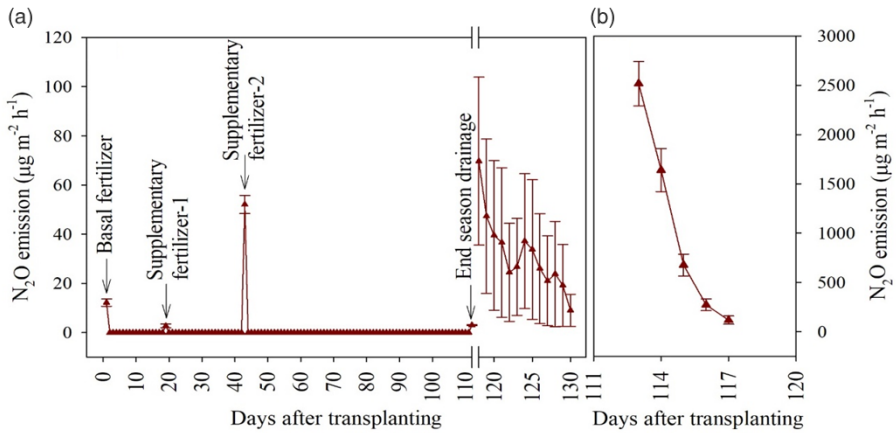

Figure 4 | (a) Temporal variation in average N_2O emission in rice paddies in all South Korea. (b) Maximum N_2O emission readily after end-season drainage.

3.4. Concentration of ammonium and nitrate

Ammonium (NH_4^+) and nitrate (NO_3^-) were simulated at different soil depths up to 50 cm from all rice paddy growing regions of South Korea (Figure 5, Tables 3 and 4). Maximum response of both NH_4^+ and NO_3^- was only observed at 0–10 cm depth in all rice paddy growing regions of South Korea. NH_4^+ increased at basal, supplementary one and two fertilizer applications. NH_4^+ decreased abruptly on the first day of end-season drainage and then decreased gradually. Total simulated NH_4^+ during the entire season was 4,929.3, 5,497.0, 5,398.6, 5,131.8, 5,225.9, 5,112.2, 5,522.3, 5,094.5, 5,253.6, 4,846.3, 4,897.0, 4,968.8, 5,165.4, 5,277.8, 4,994.1, 5,384.7, and 3,979.9 kg N ha^{-1} $season^{-1}$ recorded at sites 1, 2, 3, 4, 5, 6, 7, 8, 9, 10, 11, 12, 13, 14, 15, 16, and 17, respectively; site names are mentioned in Table 1. Throughout the season, NO_3^- was only observed after end-season drainage. NO_3^- increased rapidly for the first two days after end-season drainage and then decreased gradually upt to the last day of NO_3^- simulation. Total simulated NH_4^+ during the entire season was 580.7, 419.9, 603.2, 637.1, 607.6, 622.5, 654.7, 652.1, 602.9, 666.7, 654.3, 606.5, 662.1, 644.8, 637.7, 644.3, and 70.6 kg N ha^{-1} $season^{-1}$ recorded in 1, 2, 3, 4, 5, 6, 7, 8, 9, 10, 11, 12, 13, 14, 15, 16, and 17, respectively. Nitrous oxide is produced when nitrification and denitrification take place under aerobic and anaerobic conditions in soil, respectively (Katayanagi *et al.* 2012). Nitrification mainly regulates N_2O production in rice paddy soils as a function of NH_4^+ where it is further oxidized to NO_3^- (Pathak *et al.* 2005; Katayanagi *et al.* 2012).

3.5. Comparison of cumulative N_2O emissions

Cumulative N_2O emissions during the entire season in this study were compared with cumulative N_2O emissions of reported studies worldwide and in South Korea (Figure 6). Reported cumulative N_2O flux in rice paddies worldwide and in South Korea ranged from −0.34 to 15.27 and 0.014 to 4.2 kg-N ha^{-1} $season^{-1}$, respectively as shown in supplementary material Table S3. In this study, simulated cumulative N_2O emissions in all rice paddy growing regions of South Korea were in the range 0.68–4.29 kg-N ha^{-1} $season^{-1}$. Cumulative N_2O emissions were underestimated by 4–19% by the DNDC model (Yu *et al.* 2017, 2018).

4. CONCLUSION

Using the DNDC model, we simulated N_2O emissions in rice paddies of all rice paddy growing regions of South Korea. Reported studies in South Korea and simulated N_2O emissions in this study were strongly correlated $R^2 = 0.88$–0.90. The difference between reported and simulated N_2O emissions was 5–6%. N_2O emissions in all rice paddy growing regions of

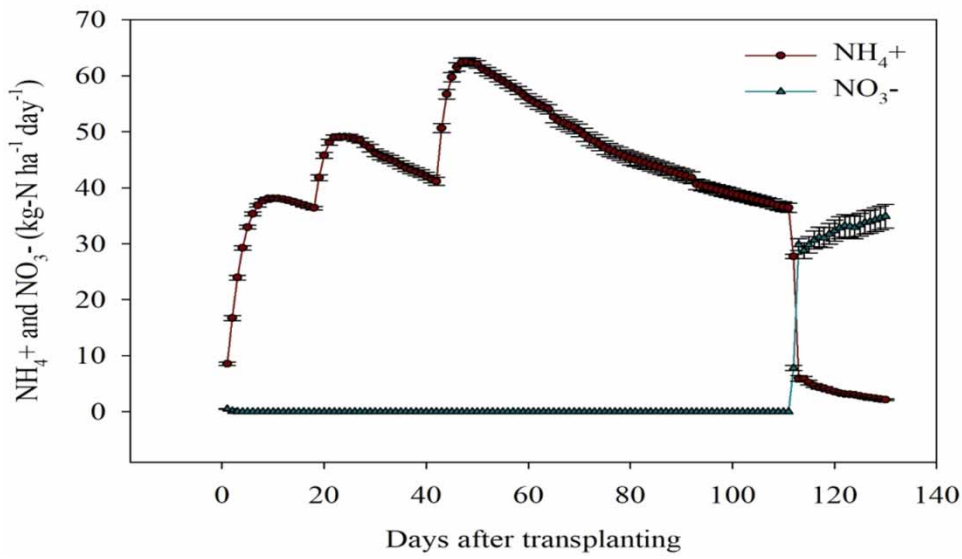

Figure 5 | Average concentration of ammonium and nitrate at 0–10 cm depth of rice paddy soils of South Korea. Error bars show standard error of the mean between all sites.

Table 3 | The average amount of ammonium (kg-N ha^{-1} $season^{-1}$) in rice paddy soils of different regions of South Korea

Soil depth (cm)	Mean	1[a]	2[a]	3[a]	4[a]	5[a]	6[a]	7[a]	8[a]	9[a]	10[a]	11[a]	12[a]	13[a]	14[a]	15[a]	16[a]	17[a]
0–10	Avg	37.9	42.3	41.5	39.5	40.2	39.3	42.5	39.2	40.4	37.3	37.7	38.2	39.7	40.6	38.4	41.4	30.6
	SE	15.7	18.1	17.1	16.6	17.5	16.6	18.3	16.8	16.3	16.2	16.3	16.8	17.4	17.9	16.5	18.1	13.8
10–20	Avg	3.4	4.9	4.4	3.5	4.2	4.0	4.2	4.0	3.9	1.4	1.6	1.7	1.8	1.6	1.7	1.5	1.8
	SE	0.6	0.2	0.3	0.4	0.2	0.3	0.3	0.3	0.4	0.7	0.8	0.8	0.9	0.8	0.9	0.9	1.1
20–30	Avg	3.7	3.8	2.7	2.2	2.7	2.5	2.7	2.5	3.4	1.0	1.1	1.2	1.3	1.2	1.2	1.4	1.2
	SE	0.4	0.2	0.2	0.2	0.2	0.2	0.2	0.2	0.3	0.4	0.5	0.5	0.5	0.5	0.5	0.4	0.5
30–40	Avg	1.7	1.4	1.3	1.0	1.3	1.2	1.2	1.2	1.6	0.5	0.5	0.6	0.6	0.5	0.5	0.7	0.6
	SE	0.2	0.1	0.1	0.1	0.1	0.1	0.1	0.1	0.2	0.2	0.2	0.2	0.2	0.2	0.2	0.2	0.2
40–50	Avg	0.8	0.7	0.6	0.5	0.6	0.5	0.6	0.5	0.8	0.2	0.2	0.3	0.3	0.3	0.2	0.3	0.3
	SE	0.10	0.05	0.05	0.04	0.05	0.04	0.05	0.04	0.08	0.06	0.07	0.08	0.08	0.08	0.07	0.06	0.09

[a]Names of different regions as listed in Table 1.

Table 4 | The average amount of nitrate (kg-N ha^{-1} $season^{-1}$) in rice paddy soils of different regions of South Korea

Soil depth (cm)	Mean	1*	2*	3*	4*	5*	6*	7*	8*	9*	10*	11*	12*	13*	14*	15*	16*	17*
0–10	Avg	4.5	3.2	4.6	4.9	4.7	4.8	5.0	5.0	4.6	5.1	5.0	4.7	5.1	5.0	4.9	5.0	0.5
	SE	11.0	8.0	11.5	12.1	11.5	11.9	12.4	12.4	11.5	12.7	12.5	11.5	12.6	12.3	12.1	12.2	2.0
10–20	Avg	0.1	0.1	0.1	0.1	0.2	0.1	0.1	0.1	0.1	0.2	0.1	0.1	0.1	0.1	0.1	0.1	0.0
	SE	0.2	0.3	0.2	0.2	0.4	0.3	0.2	0.3	0.2	0.5	0.2	0.3	0.2	0.3	0.2	0.1	0.1
20–30	Avg	0.003	0.005	0.002	0.003	0.004	0.004	0.003	0.004	0.003	0.010	0.004	0.004	0.004	0.004	0.003	0.003	0.001
	SE	0.02	0.03	0.02	0.02	0.03	0.02	0.02	0.02	0.02	0.04	0.03	0.03	0.03	0.03	0.03	0.03	0.01
30–40	Avg	0.001	0.001	0.001	0.001	0.001	0.001	0.001	0.001	0.001	0.001	0.001	0.001	0.001	0.001	0.001	0.001	0.001
	SE	0.011	0.010	0.012	0.012	0.012	0.012	0.011	0.012	0.011	0.016	0.016	0.015	0.015	0.015	0.016	0.014	0.007
40–50	Avg	0.000	0.000	0.001	0.001	0.001	0.001	0.001	0.001	0.000	0.001	0.001	0.001	0.001	0.001	0.001	0.001	0.000
	SE	0.005	0.005	0.006	0.006	0.006	0.006	0.006	0.006	0.005	0.008	0.008	0.007	0.007	0.007	0.007	0.007	0.004

*Names of different regions as listed in Table 1.

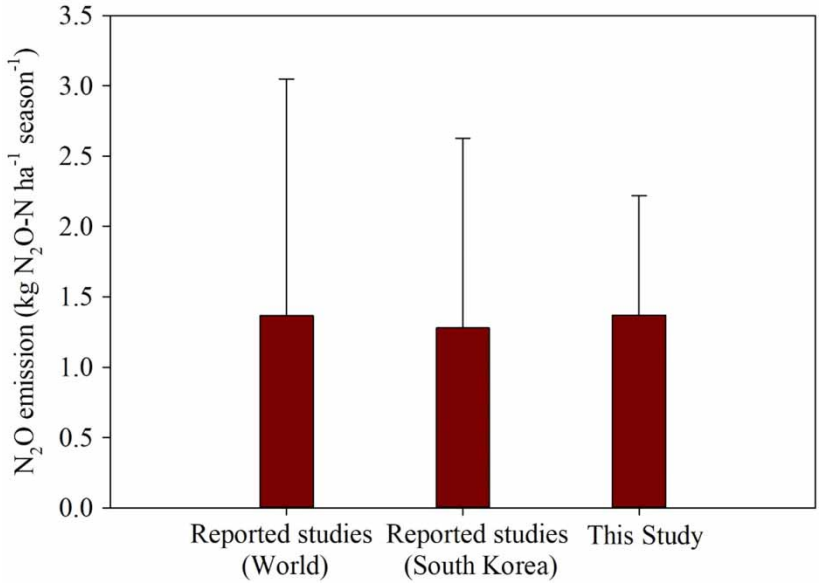

Figure 6 | Comparison of cumulative N_2O emission in rice paddies of this study with reported studies worldwide and in South Korea. Error bars show the standard deviation between N_2O fluxes from different locations.

South Korea were mainly due to NH_4^+ and NH_3- during flooding (wet period) and after end-season drainage (dry period), respectively. Minimum and maximum N_2O emissions were observed at basal fertilizer application and during end-season drainage, respectively. There was no significant difference between the reported average N_2O emissions in rice paddies worldwide, in South Korea, and that assessed in this study. This comparison of N_2O emissions reflected the reliability of N_2O estimation and our simulated results are within the range of reported studies.

ACKNOWLEDGEMENTS

The authors are thankful to the Higher Education Commission (HEC) Pakistan for providing a scholarship for Ph.D. studies at Hanyang University, Seoul, South Korea.

DATA AVAILABILITY STATEMENT

All relevant data are included in the paper or its Supplementary Information.

CONFLICT OF INTEREST

The authors declare there is no conflict.

REFERENCES

Abbas, T., Zhou, H., Zhang, Q., Li, Y., Liang, Y., Di, H. & Zhao, Y. 2019 Anammox co-fungi accompanying denitrifying bacteria are the thieves of the nitrogen cycle in paddy-wheat crop rotated soils. *Environment International* **130**, 104913.

Abdalla, M., Jones, M., Yeluripati, J., Smith, P., Burke, J. & Williams, M. 2010 Testing DayCent and DNDC model simulations of N_2O fluxes and assessing the impacts of climate change on the gas flux and biomass production from a humid pasture. *Atmospheric Environment* **44**, 2961–2970.

Abdalla, M., Song, X., Ju, X., Topp, C. F. & Smith, P. 2020a Calibration and validation of the DNDC model to estimate nitrous oxide emissions and crop productivity for a summer maize-winter wheat double cropping system in Hebei, China. *Environmental Pollution (Barking, Essex: 1987)* **262**, 114199–114199.

Abdalla, M., Song, X., Ju, X., Topp, C. F. & Smith, P. 2020b Calibration and validation of the DNDC model to estimate nitrous oxide emissions and crop productivity for a summer maize-winter wheat double cropping system in Hebei, China. *Environmental Pollution* **262**, 114199.

Adviento-Borbe, M. A., Necita Padilla, G., Pittelkow, C. M., Simmonds, M., Van Kessel, C. & Linquist, B. 2015 Methane and nitrous oxide emissions from flooded rice systems following the end-of-season drain. *Journal of Environmental Quality* **44**, 1071–1079.

Ali, M. A., Lee, C. H. & Kim, P. J. 2008 Effect of silicate fertilizer on reducing methane emission during rice cultivation. *Biology and Fertility of Soils* **44**, 597–604.

Babu, Y. J., Li, C., Frolking, S., Nayak, D. R. & Adhya, T. 2006 Field validation of DNDC model for methane and nitrous oxide emissions from rice-based production systems of India. *Nutrient Cycling in Agroecosystems* **74**, 157–174.

Bashir, M. A., Liu, J., Geng, Y., Wang, H., Pan, J., Zhang, D., Rehim, A., Aon, M. & Liu, H. 2020 Co-culture of rice and aquatic animals: an integrated system to achieve production and environmental sustainability. *Journal of Cleaner Production* **249**, 119310.

Berger, S., Jang, I., Seo, J., Kang, H. & Gebauer, G. 2013a A record of N_2O and CH 4 emissions and underlying soil processes of Korean rice paddies as affected by different water management practices. *Biogeochemistry* **115**, 317–332.

Berger, S., Jang, I., Seo, J., Kang, H. & Gebauer, G. 2013b A record of N_2O and CH 4 emissions and underlying soil processes of Korean rice paddies as affected by different water management practices. *Biogeochemistry* **115**, 317–332.

Bhanja, S. N., Wang, J., Shrestha, N. K. & Zhang, X. 2019 Microbial kinetics and thermodynamic (MKT) processes for soil organic matter decomposition and dynamic oxidation-reduction potential: model descriptions and applications to soil N_2O emissions. *Environmental Pollution* **247**, 812–823.

Brenzinger, K., Drost, S. M., Korthals, G. & Bodelier, P. L. 2018 Organic residue amendments to modulate greenhouse gas emissions from agricultural soils. *Frontiers in Microbiology* **9**, 3035.

Brown, L., Jarvis, S. & Headon, D. 2001 A farm-scale basis for predicting nitrous oxide emissions from dairy farms. *Nutrient Cycling in Agroecosystems* **60**, 149–158.

Cai, Z. 2012 Greenhouse gas budget for terrestrial ecosystems in China. *Science China Earth Sciences* **55**, 173–182.

Cai, Z., Sawamoto, T., Li, C., Kang, G., Boonjawat, J., Mosier, A., Wassmann, R. & Tsuruta, H. 2003 Field validation of the DNDC model for greenhouse gas emissions in East Asian cropping systems. *Global Biogeochemical Cycles* **17**, 1107.

Camarotto, C., Dal Ferro, N., Piccoli, I., Polese, R., Furlan, L., Chiarini, F. & Morari, F. 2018 Conservation agriculture and cover crop practices to regulate water, carbon and nitrogen cycles in the low-lying Venetian plain. *Catena* **167**, 236–249.

Chen, H., Li, L., Luo, X., Li, Y., Liu, D. L., Zhao, Y., Feng, H. & Deng, J. 2019a Modeling impacts of mulching and climate change on crop production and N_2O emission in the Loess Plateau of China. *Agricultural and Forest Meteorology* **268**, 86–97.

Chen, M., Zhou, X.-F., Yu, Y.-Q., Liu, X., Zeng, R. J.-X., Zhou, S.-G. & He, Z. 2019b Light-driven nitrous oxide production via autotrophic denitrification by self-photosensitized *Thiobacillus denitrificans*. *Environment International* **127**, 353–360.

Chun, J., Shim, K., Min, S. & Wang, Q. 2016 Methane mitigation for flooded rice paddy systems in South Korea using a process-based model. *Paddy and Water Environment* **14**, 123–129.

Cui, G. & Wang, J. 2019 Improving the DNDC biogeochemistry model to simulate soil temperature and emissions of nitrous oxide and carbon dioxide in cold regions. *Science of the Total Environment* **687**, 61–70.

Duan, P., Song, Y., Li, S. & Xiong, Z. 2019 Responses of N_2O production pathways and related functional microbes to temperature across greenhouse vegetable field soils. *Geoderma* **355**, 113904.

Dutta, B., Grant, B. B., Congreves, K. A., Smith, W. N., Wagner-Riddle, C., VanderZaag, A. C., Tenuta, M. & Desjardins, R. L. 2018 Characterising effects of management practices, snow cover, and soil texture on soil temperature: model development in DNDC. *Biosystems Engineering* **168**, 54–72.

Fahad, S., Noor, M., Adnan, M., Khan, M. A., Rahman, I. U., Alam, M., Khan, I. A., Ullah, H., Mian, I. A. & Hassan, S. 2019 Abiotic stress and rice grain quality. In: Hasanuzzaman, M., Fujita, M., Nahar, K., Biswas, J. K. (Eds).; Woodhead Publishing: Cambridge, UK, pp. 571–583. *Advances in Rice Research for Abiotic Stress Tolerance*. Woodhead Publishing: Cambridge, UK, pp. 571–583.

Fan, C., Duan, P., Zhang, X., Shen, H., Chen, M. & Xiong, Z. 2020 Mechanisms underlying the mitigation of both N_2O and NO emissions with field-aged biochar in an anthrosol. *Geoderma* **364**, 114178.

Fumoto, T., Kobayashi, K., Li, C., Yagi, K. & Hasegawa, T. 2008 Revising a process-based biogeochemistry model (DNDC) to simulate methane emission from rice paddy fields under various residue management and fertilizer regimes. *Global Change Biology* **14**, 382–402.

Fumoto, T., Yanagihara, T., Saito, T. & Yagi, K. 2010 Assessment of the methane mitigation potentials of alternative water regimes in rice fields using a process-based biogeochemistry model. *Global Change Biology* **16**, 1847–1859.

Gaillard, R., Duval, B. D., Osterholz, W. R. & Kucharik, C. J. 2016 Simulated effects of soil texture on nitrous oxide emission factors from corn and soybean agroecosystems in Wisconsin. *Journal of Environmental Quality* **45**, 1540–1548.

Gaillard, R. K., Jones, C. D., Ingraham, P., Collier, S., Izaurralde, R. C., Jokela, W., Osterholz, W., Salas, W., Vadas, P. & Ruark, M. D. 2018 Underestimation of N_2O emissions in a comparison of the DayCent, DNDC, and EPIC models. *Ecological Applications* **28**, 694–708.

Giguere, A. T., Taylor, A. E., Myrold, D. D., Mellbye, B. L., Sayavedra-Soto, L. A. & Bottomley, P. J. 2018 Nitrite-oxidizing activity responds to nitrite accumulation in soil. *FEMS Microbiology Ecology* **94**, fiy008.

Giltrap, D., Yeluripati, J., Smith, P., Fitton, N., Smith, W., Grant, B., Dorich, C. D., Deng, J., Topp, C. F. & Abdalla, M. 2020 Global research alliance N_2O chamber methodology guidelines: summary of modeling approaches. *Journal of Environmental Quality* **49**, 1168–1185.

Goglio, P., Smith, W., Grant, B., Desjardins, R., Gao, X., Hanis, K., Tenuta, M., Campbell, C., McConkey, B. & Nemecek, T. 2018 A comparison of methods to quantify greenhouse gas emissions of cropping systems in LCA. *Journal of Cleaner Production* **172**, 4010–4017.

Gutierrez, J., Kim, S. Y. & Kim, P. J. 2013 Effect of rice cultivar on CH_4 emissions and productivity in Korean paddy soil. *Field Crops Research* **146**, 16–24.

Haque, M. M., Biswas, J., Kim, S. & Kim, P. 2016 Suppressing methane emission and global warming potential from rice fields through intermittent drainage and green biomass amendment. *Soil Use and Management* **32**, 72–79.

He, W., Grant, B. B., Smith, W. N., VanderZaag, A. C., Piquette, S., Qian, B., Jing, Q., Rennie, T. J., Bélanger, G. & Jégo, G. 2019 Assessing alfalfa production under historical and future climate in eastern Canada: DNDC model development and application. *Environmental Modelling & Software* **122**, 104540.

Hu, H.-W., Chen, D. & He, J.-Z. 2015 Microbial regulation of terrestrial nitrous oxide formation: understanding the biological pathways for prediction of emission rates. *FEMS Microbiology Reviews* **39**, 729–749.

IPCC 2007 *Climate Change 2007: The Physical Science Basis. Contribution of Working Group I to the Fourth Assessment Report of the Intergovernmental Panel on Climate Change*. IPCC Secretariat, Geneva, Switzerland.

Ishii, S., Ikeda, S., Minamisawa, K. & Senoo, K. 2009 Nitrogen cycling in rice paddy environments: past achievements and future challenges. *Microbes and Environments* **26**, 282–292.

Jiang, Q., Qi, Z., Madramootoo, C. A., Smith, W., Abbasi, N. A. & Zhang, T. 2020 Comparison of RZWQM2 and DNDC models to simulate greenhouse gas emissions under combined inorganic/organic fertilization in a subsurface-drained field. *Transactions of the ASABE* **63**, 771–787.

Jiang, R., Yang, J., Drury, C., He, W., Smith, W., Grant, B., He, P. & Zhou, W. 2021 Assessing the impacts of diversified crop rotation systems on yields and nitrous oxide emissions in Canada using the DNDC model. *Science of The Total Environment* **759**, 143433.

Katayanagi, N., Furukawa, Y., Fumoto, T. & Hosen, Y. 2012 Validation of the DNDC-Rice model by using CH_4 and N_2O flux data from rice cultivated in pots under alternate wetting and drying irrigation management. *Soil Science and Plant Nutrition* **58**, 360–372.

Kim, S. Y., Gutierrez, J. & Kim, P. J. 2012 Considering winter cover crop selection as green manure to control methane emission during rice cultivation in paddy soil. *Agriculture, Ecosystems & Environment* **161**, 130–136.

Kim, S. Y., Lee, C. H., Gutierrez, J. & Kim, P. J. 2013 Contribution of winter cover crop amendments on global warming potential in rice paddy soil during cultivation. *Plant and Soil* **366**, 273–286.

Kim, G.-Y., Gutierrez, J., Jeong, H.-C., Lee, J.-S., Haque, M. M. & Kim, P. J. 2014a Effect of intermittent drainage on methane and nitrous oxide emissions under different fertilization in a temperate paddy soil during rice cultivation. *Journal of the Korean Society for Applied Biological Chemistry* **57**, 229–236.

Kim, S. Y., Pramanik, P., Bodelier, P. L. & Kim, P. J. 2014b Cattle manure enhances methanogens diversity and methane emissions compared to swine manure under rice paddy. *PLoS One* **9**, e113593.

Kim, S., Lee, S., McCormick, M., Kim, J. G. & Kang, H. 2016a Microbial community and greenhouse gas fluxes from abandoned rice paddies with different vegetation. *Microbial Ecology* **72**, 692–703.

Kim, S. Y., Gutierrez, J. & Kim, P. J. 2016b Unexpected stimulation of CH_4 emissions under continuous no-tillage system in mono-rice paddy soils during cultivation. *Geoderma* **267**, 34–40.

Kimura, M. 2000 Anaerobic microbiology in waterlogged rice fields. *Soil Biochemistry* **10**, 35–138.

KMA 2019 *Monthly Report of Automatic Weather System Data From January to December*. Korea Meteorological Administration (KMA), Seoul, Korea.

KOSIS 2019 *Statistical Information Service (KOSIS) Report*. Korea. Available from: http://kosis.kr/eng/.

Lee, C. H., Do Park, K., Jung, K. Y., Ali, M. A., Lee, D., Gutierrez, J. & Kim, P. J. 2010 Effect of Chinese milk vetch (Astragalus sinicus L.) as a green manure on rice productivity and methane emission in paddy soil. *Agriculture, Ecosystems & Environment* **138**, 343–347.

Lee, E., Han, S.-K. & Im, S. 2019 Performance analysis of log extraction by a small shovel operation in steep forests of South Korea. *Forests* **10**, 585.

Li, C., Qiu, J., Frolking, S., Xiao, X., Salas, W., Moore III., B., Boles, S., Huang, Y. & Sass, R. 2002 Reduced methane emissions from large-scale changes in water management of China's rice paddies during 1980–2000. *Geophysical Research Letters* **29**, 33-31-33-34.

Li, S., Zheng, X., Zhang, W., Han, S., Deng, J., Wang, K., Wang, R., Yao, Z. & Liu, C. 2019 Modeling ammonia volatilization following the application of synthetic fertilizers to cultivated uplands with calcareous soils using an improved DNDC biogeochemistry model. *Science of the Total Environment* **660**, 931–946.

Liao, B., Wu, X., Yu, Y., Luo, S., Hu, R. & Lu, G. 2020 Effects of mild alternate wetting and drying irrigation and mid-season drainage on CH_4 and N_2O emissions in rice cultivation. *Science of The Total Environment* **698**, 134212.

Liu, H., Ding, Y., Zhang, Q., Liu, X., Xu, J., Li, Y. & Di, H. 2019a Heterotrophic nitrification and denitrification are the main sources of nitrous oxide in two paddy soils. *Plant and Soil* **445**, 39–53.

Liu, X., Zhou, T., Liu, Y., Zhang, X., Li, L. & Pan, G. 2019b Effect of mid-season drainage on CH_4 and N_2O emission and grain yield in rice ecosystem: a meta-analysis. *Agricultural Water Management* **213**, 1028–1035.

Macdonald, D. S. & Clark, D. N. 2018 *The Koreans: Contemporary Politics and Society*. Boulder, CO: Westview, New York, Routledge.

Majumdar, D. 2013 Biogeochemistry of N_2O uptake and consumption in submerged soils and rice fields and implications in climate change. *Critical Reviews in Environmental Science and Technology* **43**, 2653–2684.

Massara, T. M., Solís, B., Guisasola, A., Katsou, E. & Baeza, J. A. 2018 Development of an ASM2d-N_2O model to describe nitrous oxide emissions in municipal WWTPs under dynamic conditions. *Chemical Engineering Journal* **335**, 185–196.

Neszmelyi, G. I. 2017 *The Main Characteristics of The South Korean Agriculture*. Economic and Local Aspects of Rural Development, Szent Istvan University, Budapest, Hungary, pp. 31–43.

Ogle, S. M., Butterbach-Bahl, K., Cardenas, L., Skiba, U. & Scheer, C. 2020 From research to policy: optimizing the design of a national monitoring system to mitigate soil nitrous oxide emissions. *Current Opinion in Environmental Sustainability* **47**, 28–36.

Ok, Y. S., Kim, S.-C., Kim, D.-K., Skousen, J. G., Lee, J.-S., Cheong, Y.-W., Kim, S.-J. & Yang, J. E. 2011 Ameliorants to immobilize Cd in rice paddy soils contaminated by abandoned metal mines in Korea. *Environmental Geochemistry and Health* **33**, 23–30.

Osozawa, S. & Kubota, T. 1987 A simple method to determine gas diffusion coefficient in soil. *Japanese Journal of Soil Science and Plant Nutrition (Japan)* **58**, 528–535.

Pandey, A., Vu, D. Q., Bui, T. P. L., Mai, T. L. A., Jensen, L. S. & de Neergaard, A. 2014 Organic matter and water management strategies to reduce methane and nitrous oxide emissions from rice paddies in Vietnam. *Agriculture, Ecosystems & Environment* **196**, 137–146.

Pandey, A., Dou, F., Morgan, C. L., Guo, J., Deng, J. & Schwab, P. 2021 Modeling organically fertilized flooded rice systems and its long-term effects on grain yield and methane emissions. *Science of The Total Environment* **755**, 142578.

Pathak, H., Li, C. & Wassmann, R. 2005 Greenhouse gas emissions from Indian rice fields: calibration and upscaling using the DNDC model. *Biogeosciences* **2**, 113–123.

Penning de Vries, F. W. T., Jansen, D. M., ten Berge, H. F. M. & Bakema, A. 1989 Simulation of ecophysiological processes of growth of several annual crops. Simulation Monographs. Centre for Agricultural Publishing and Documentation (Pudoc). Wageningen, Netherlands.

Pramanik, P. & Kim, P. J. 2014 Mitigate CH_4 emission by suppressing methanogen activity in rice paddy soils using ethylenediaminetetraacetic acid (EDTA). *Geoderma* **219**, 58–62.

Pramanik, P., Haque, M. M. & Kim, P. J. 2013 Effect of nodule formation in roots of hairy vetch (*Vicia villosa*) on methane and nitrous oxide emissions during succeeding rice cultivation. *Agriculture, Ecosystems & Environment* **178**, 51–56.

Pramanik, P., Haque, M. M., Kim, S. Y. & Kim, P. J. 2014 C and N accumulations in soil aggregates determine nitrous oxide emissions from cover crop treated rice paddy soils during fallow season. *Science of the Total Environment* **490**, 622–628.

Qin, H., Xing, X., Tang, Y., Zhu, B., Wei, X., Chen, X. & Liu, Y. 2020 Soil moisture and activity of nitrite- and nitrous oxide-reducing microbes enhanced nitrous oxide emissions in fallow paddy soils. *Biology and Fertility of Soils* **56**, 53–67.

Rafique, R., Kumar, S., Luo, Y., Xu, X., Li, D. & Zhang, W. 2014 Estimation of greenhouse gases (N_2O, CH_4 and CO_2) from no-till cropland under increased temperature and altered precipitation regime: a DAYCENT model approach. *Global and Planetary Change* **118**, 106–114.

Rolston, D. E. 1986 Gas flux. In A. Klute (ed.), Methods of Soil Analysis, Part One. Physical and Mineralogical Methods. Madison: SSSA Book Ser. 5, pp. 1103–1119.

Shen, J., Treu, R., Wang, J., Nicholson, F., Bhogal, A. & Thorman, R. 2018 Modeling nitrous oxide emissions from digestate and slurry applied to three agricultural soils in the United Kingdom: fluxes and emission factors. *Environmental Pollution* **243**, 1952–1965.

Shen, J., Melaku, N. D., Treu, R. & Wang, J. 2019 Inventories of methane and nitrous oxide emissions from animal and crop farms of 69 municipalities in Alberta, Canada. *Journal of Cleaner Production* **234**, 895–911.

Tang, J., Wang, J., Li, Z., Wang, S. & Qu, Y. 2018 Effects of irrigation regime and nitrogen fertilizer management on CH_4, N_2O and CO_2 emissions from saline–alkaline paddy fields in Northeast China. *Sustainability* **10**, 475.

Tian, Z., Niu, Y., Fan, D., Sun, L., Ficsher, G., Zhong, H., Deng, J. & Tubiello, F. N. 2018 Maintaining rice production while mitigating methane and nitrous oxide emissions from paddy fields in China: evaluating tradeoffs by using coupled agricultural systems models. *Agricultural Systems* **159**, 175–186.

Wang, N., Chang, Z.-Z., Xue, X.-M., Yu, J.-G., Shi, X.-X., Ma, L. Q. & Li, H.-B. 2017 Biochar decreases nitrogen oxide and enhances methane emissions via altering microbial community composition of anaerobic paddy soil. *Science of the Total Environment* **581**, 689–696.

Wang, C., Amon, B., Schulz, K. & Mehdi, B. 2021a Factors that influence nitrous oxide emissions from agricultural soils as well as their representation in simulation models: a review. *Agronomy* **11**, 770.

Wang, Z., Zhang, X., Liu, L., Wang, S., Zhao, L., Wu, X., Zhang, W. & Huang, X. 2021b Estimates of methane emissions from Chinese rice fields using the DNDC model. *Agricultural and Forest Meteorology* **303**, 108368.

Wang, C., Zhao, J., Gao, Z., Feng, Y., Laraib, I., Chen, F. & Chu, Q. 2022 Exploring wheat-based management strategies to balance agricultural production and environmental sustainability in a wheat–maize cropping system using the DNDC model. *Journal of Environmental Management* **307**, 114445.

Wei, X., Hu, Y., Peng, P., Zhu, Z., Atere, C. T., O'Donnell, A. G., Wu, J. & Ge, T. 2017 Effect of P stoichiometry on the abundance of nitrogen-cycle genes in phosphorus-limited paddy soil. *Biology and Fertility of Soils* **53**, 767–776.

Wei, X., Zhu, Z., Wei, L., Wu, J. & Ge, T. 2019 Biogeochemical cycles of key elements in the paddy-rice rhizosphere: microbial mechanisms and coupling processes. *Rhizosphere* **10**, 100145.

Wu, X. & Zhang, A. 2014 Comparison of three models for simulating N_2O emissions from paddy fields under water-saving irrigation. *Atmospheric Environment* **98**, 500–509.

Wu, K., Gong, P., Bai, W., Zhang, Z., Wei, Z., Yu, C., Song, Y., Xue, Y. & Zhang, L. 2022 Effect of mixed inhibitor application on N_2O production pathways in paddy soil. *Journal of Soils and Sediments* **22**, 1–11.

Xing, G., Zhao, X., Xiong, Z., Yan, X., Xu, H., Xie, Y. & Shi, S. 2009 Nitrous oxide emission from paddy fields in China. *Acta Ecologica Sinica* **29**, 45–50.

Xu, X., Liu, X., Li, Y., Ran, Y., Liu, Y., Zhang, Q., Li, Z., He, Y., Xu, J. & Di, H. 2017 Legacy effects of simulated short-term climate change on ammonia oxidisers, denitrifiers, and nitrous oxide emissions in an acid soil. *Environmental Science and Pollution Research* **24**, 11639–11649.

Xu, X., He, C., Yuan, X., Zhang, Q., Wang, S., Wang, B., Guo, X. & Zhang, L. 2020 Rice straw biochar mitigated more N2O emissions from fertilized paddy soil with higher water content than that derived from ex situ biowaste. *Environmental Pollution* **263**, 114477.

Yao, Y., Zeng, K. & Song, Y. 2020 Biological nitrification inhibitor for reducing N_2O and NH_3 emissions simultaneously under root zone fertilization in a Chinese rice field. *Environmental Pollution* **264**, 114821.

Yin, S., Zhang, X., Lyu, J., Zhi, Y., Chen, F., Wang, L., Liu, C. & Zhou, S. 2020 Carbon sequestration and emissions mitigation in paddy fields based on the DNDC model: a review. *Artificial Intelligence in Agriculture* **4**, 140–149.

You, S. D. 2009 Housing Finance Mechanisms in the Republic of Korea. UN-HABITAT, Narobi.

Yu, Y., Tao, H., Jia, H. & Zhao, C. 2017 Impact of plastic mulching on nitrous oxide emissions in China's arid agricultural region under climate change conditions. *Atmospheric Environment* **158**, 76–84.

Yu, Y., Tao, H., Yao, H. & Zhao, C. 2018 Assessment of the effect of plastic mulching on soil respiration in the arid agricultural region of China under future climate scenarios. *Agricultural and Forest Meteorology* **256–257**, 1–9.

Yue, Q., Cheng, K., Ogle, S., Hillier, J., Smith, P., Abdalla, M., Ledo, A., Sun, J. & Pan, G. 2019 Evaluation of four modelling approaches to estimate nitrous oxide emissions in China's cropland. *Science of the Total Environment* **652**, 1279–1289.

Zhang, Y. & Niu, H. 2016 The development of the DNDC plant growth sub-model and the application of DNDC in agriculture: a review. *Agriculture, Ecosystems & Environment* **230**, 271–282.

Zhang, M., Wang, W., Tang, L., Heenan, M. & Xu, Z. 2018a Effects of nitrification inhibitor and herbicides on nitrification, nitrite and nitrate consumptions and nitrous oxide emission in an Australian sugarcane soil. *Biology and Fertility of Soils* **54**, 697–706.

Zhang, W., Li, Y., Zhu, B., Zheng, X., Liu, C., Tang, J., Su, F., Zhang, C., Ju, X. & Deng, J. 2018b A process-oriented hydro-biogeochemical model enabling simulation of gaseous carbon and nitrogen emissions and hydrologic nitrogen losses from a subtropical catchment. *Science of The Total Environment* **616**, 305–317.

Zhang, S., Liu, F., Luo, P., Xiao, R., Chen, J., Chen, L. & Wu, J. 2019 Does rice straw application reduce N_2O emissions from surface flow constructed wetlands for swine wastewater treatment? *Chemosphere* **226**, 273–281.

Zhao, Z., Cao, L., Deng, J., Sha, Z., Chu, C., Zhou, D., Wu, S. & Lv, W. 2020 Modeling CH_4 and N_2O emission patterns and mitigation potential from paddy fields in Shanghai, China with the DNDC model. *Agricultural Systems* **178**, 102743.

Zuo, J., Hu, H., Fu, Q., Zhu, J., Zheng, H., Mo, M. & Tu, A. 2022 Responses of N_2O production and abundances of associated microorganisms to soil profiles and water regime in two paddy soils. *Agronomy* **12**, 743.

Žurovec, O., Wall, D. P., Brennan, F. P., Krol, D. J., Forrestal, P. J. & Richards, K. G. 2021 Increasing soil pH reduces fertiliser derived N_2O emissions in intensively managed temperate grassland. *Agriculture, Ecosystems & Environment* **311**, 107319.

First received 21 February 2022; accepted in revised form 19 August 2022. Available online 27 August 2022